Neuroinflammation as potential precursor of leukoencephalopathy in early-stage breast cancer patients: A cross-sectional PET-MRI study

Gwen Schroyen [a,b,c,1], Charlotte Sleurs [a,b,d,*,1], Emilie Bartsoen [d], Dirk Smeets [e], Donatienne van Weehaeghe [f,g], Koen Van Laere [a,b,c,f,g], Ann Smeets [b,d,h], Sabine Deprez [a,b,c], Stefan Sunaert [a,c,i]

a Leuven Brain Institute, KU Leuven, 3000, Leuven, Belgium
b Leuven Cancer Institute, KU Leuven, 3000, Leuven, Belgium
c Department of Imaging and Pathology, KU Leuven, 3000, Leuven, Belgium
d Department of Oncology, KU Leuven, 3000, Leuven, Belgium
e icometrix, 3012, Leuven, Belgium
f Nuclear Medicine, University Hospitals Leuven, 3000, Leuven, Belgium
g Department of Nuclear Medicine and Molecular Imaging, KU Leuven, 3000, Leuven, Belgium
h Surgical Oncology, University Hospitals Leuven, 3000, Leuven, Belgium
i Radiology, University Hospitals Leuven, 3000, Leuven, Belgium

ARTICLE INFO

ABSTRACT

Background: Although chemotherapy-induced leukoencephalopathy has been described in case and cohort studies, literature remains inconclusive about its prevalence and mechanisms. Therefore, we investigated the presence of leukoencephalopathy after multiagent chemotherapy in women treated for breast cancer and potential underlying neuroinflammatory processes.

Methods: In this exploratory study, 15 chemotherapy-treated and 15 age-matched chemotherapy-naïve patients with early-stage breast cancer, as well as 15 healthy controls underwent simultaneous PET-MR neuroimaging, including T1-weighted MPRAGE, T2-weighted FLAIR and dynamic PET with the 18-kDA translocator protein (TSPO) radioligand [18F]DPA-714. Total and regional (juxtacortical, periventricular, deep white matter and infratentorial) lesion burden were compared between the groups with one-way ANOVA. With paired t-tests, [18F] DPA-714 volume of distribution [V_T, including partial volume correction (PVC)] in lesioned and normal appearing white matter (NAWM) were compared within subjects, to investigate inflammation. Finally, two general linear models were used to examine the predictive values of neurofilament light-chain (NfL) serum levels on (1) total lesion burden or (2) PVC [18F]DPA-714 V_T of lesions showing elevated inflammation.

Results: No significant differences were found in total or localized lesion burden. However, significantly higher (20–45%) TSPO uptake was observed in juxtacortical lesions ($p \leq 0.008$, $t \geq 3.90$) compared to NAWM in both cancer groups, but only persisted for chemotherapy-treated patients after PVC ($p = 0.005$, $t = 4.30$). NfL serum levels were not associated with total lesion volume or tracer uptake in juxtacortical lesions.

Conclusion: This multimodal neuroimaging study suggests that neuroinflammatory processes could be involved in the development of juxtacortical, but not periventricular or deep white matter, leukoencephalopathy shortly after chemotherapy for early-stage breast cancer.

1. Introduction

In western women, breast cancer is the most common type of cancer [1]. As the implementation of chemotherapy has substantially increased survival rates of early-stage breast cancer, potential long-term side-effects have become increasingly important. One of such potential sequelae involves neural damage with related cognitive symptoms, often termed as "chemobrain" or cancer-related cognitive impairment [2]. Up to 78% of women treated for early-stage breast cancer with adjuvant chemotherapy can show cognitive deficits, mainly affecting domains of executive functioning, (working) memory and processing speed, even without the presence of (brain) metastasis [2,3]. These deficits are observed months [4,5] up to years after the cessation of chemotherapy [6–8]. Although these deficits are mostly subtle, they can have a detrimental effect on the patient's daily life [9]. However, the underlying mechanisms remain largely under investigation [10].

Chemotherapeutic agents could directly induce neuronal and axonal damage. Axons represent the connections between neurons, ensuring rapid communication because of myelin sheaths allowing efficient transmission of electrical impulses [11]. Hence, demyelination can easily lead to delayed communication between neurons and secondary axonal degeneration, which can result in decreased processing speed for instance Ref. [12]. In rodents, Gibson et al. (2019), found decreased oligodendrocyte proliferation and maturation as well as thinned myelin sheaths after chemotherapy [13]. To examine such damage to the white matter in humans, several investigation methods can be employed. Firstly, promising blood markers such as neurofilament light-chain (NfL) exist. This marker demonstrates high prognostic and diagnostic accuracy for axonal damage in cortical neurodegenerative disorders [14]. Furthermore, NfL appears to correlate with lesion burden in multiple sclerosis (MS) patients [15]. With regard to oncological populations, NfL increases after chemotherapy in a dose-dependent manner in early-stage breast cancer patients [16] and is elevated compared to chemotherapy-naïve or healthy women [17], suggesting its potential as a marker for chemotherapy-induced neuronal damage. Secondly, more direct neural-microstructure and -function can be estimated *in vivo* by neuroimaging techniques such as magnetic resonance imaging (MRI). In early-stage breast cancer patients, altered white matter microstructural organization (possibly suggesting demyelination) has repeatedly been reported after chemotherapy using diffusion weighted MR imaging [4, 18]. However, specific MR sequences estimating myelination levels (e.g. myelin water imaging) are only sparsely investigated, showing null results to date [19]. In order to visualize white matter disease [e.g. MS], T2-weighted-Fluid-Attenuated Inversion Recovery (FLAIR) imaging is most often used, which shows white matter lesions (WMLs) as hyperintense regions [12]. High-dose chemotherapy is known to potentially cause MS-mimicking WMLs observable via FLAIR, or so-called leukoencephalopathy [20,21]. Additionally, post-mortem brain autopsies of former (metastatic) cancer patients treated with high-dose chemotherapy revealed demyelination in areas that showed WMLs on T2-weighted scans *in vivo* [22]. Only few studies have examined the prevalence of leukoencephalopathy in early-stage breast cancer patients. These studies either did not encounter treatment-associated leukoencephalopathy at all or only observed higher lesion load in patients showing neurologic symptoms [7,20]. This could partly be explained by different cancer types or stages and consequently other treatment regimens, as well as the heterogeneity in forms of observed lesions (for instance multifocal punctuate lesions are less easily detected). However, aforementioned studies often applied visual rating of the WMLs, according to a neuroradiological scale (e.g. Fazekas). In contrast, volumetric lesion analyses could be more sensitive to detect subtle changes in lesion load after chemotherapy but have only limitedly been assessed in early-stage breast cancer patients [23].

Besides directly induced cell death and/or demyelination, the underlying pathology of chemotherapy-induced WMLs can involve multiple indirect processes as well, including microvascular changes, vasogenic and cytotoxic edema, oxidative stress and inflammatory pathways [24,25]. Especially this last phenomenon has gained attention recently, with histological rodent studies demonstrating changes in brain microglial levels after chemotherapy [26]. *In vivo*, positron emission tomography (PET) imaging using radioligands sensitive for the 18 kDA translocator protein (TSPO) is one potential method to visualize neuroinflammation, as TSPO expression is increased when microglia are activated [27,28]. Increased uptake of this tracer has repeatedly been found in neurodegenerative diseases characterized by immune system activation (e.g. Parkinson or Amyotrophic Lateral Sclerosis) [29,30]. Recently, our group demonstrated that shortly after ending chemotherapy, increases in relative brain TSPO binding also occur in breast cancer patients, which were associated with cognitive outcomes [17].

Gibson and Monje (2019) suggested chemotherapy to induce activation of microglia, resulting in fewer oligodendrocyte precursor cells (OPC) and decreased NPC proliferation, leading to secondary demyelination [13]. In line with this hypothesis, rodent research has shown that neuroinflammation after chemotherapy can modulate myelin structure and myelination [31]. Moreover, early on in MS, a recent study found a positive association between a microglia-related protein and NfL in cerebrospinal fluid (CSF), underscoring the relationship between inflammatory and axonal degenerative processes [32]. In concordance, we observed local increases in neuroinflammation after chemotherapy for breast cancer to be associated with lower average fiber cross-section of the corpus callosum [17]. Reactive microglia, or more generally neuroinflammatory processes, might be initiating toxic cascades involving decreased cell proliferation and/or demyelination, of which WMLs might be an observable sequela. Recent PET studies in MS patients partly support this hypothesis, in which binding of radioligands specific for inflammatory cells (e.g. TSPO) showed significantly higher in WMLs (i. e. hyperintensities) and correlated positively with the size of the lesioned area [33,34]. This was also validated in post-mortem brain tissue samples of MS patients [35].

Based on these findings, we investigated whether an inflammatory pathway could be involved in chemotherapy-induced leukoencephalopathy. We first assessed whether WML load was higher in patients treated with chemotherapy. Second, we investigated whether focal tracer uptake was higher in lesioned areas compared to the normal-appearing white matter (NAWM). Finally, we addressed if inflammation levels in "active inflammatory WMLs" (i.e. WMLs with higher TSPO levels than NAWM) were associated with NfL serum concentrations.

2. Methods

2.1. Participants

This exploratory cohort study recruited women who were diagnosed with early-stage breast cancer at the University Hospitals of Leuven and healthy women between 2017 and 2020. Details on the participants demographic and clinical characteristics are provided in Table 1 and were described earlier [17]. In total, 45 women participated in this study; 15 patients who had received chemotherapy (C+) (4 rounds of epirubicin 90 mg/m^2 + cyclophosphamide 600 mg/m^2 and 4–12 rounds of paclitaxel 80 mg/m^2), 15 chemotherapy-naïve control patients (C-) and 15 age-matched healthy control women. Neuroimaging acquisition and blood sampling took place on the same day before the administration of anti-hormone therapy or radiotherapy. For chemotherapy-naïve patients, data collection took place 26 ± 17 days after surgery. For chemotherapy-treated patients, depending on neo-adjuvant or adjuvant chemotherapy regimen, data collection took place 36 ± 12 days after surgery or last administration of chemotherapy, respectively. Participants were excluded if they were older than 65 years, pregnant/breast-feeding, showed signs of metastatic cancer (except for lymph nodes), had received former cancer treatment, had a psychiatric or neurological illness, chronic systemic steroid use, or intellectual disability. In addition, participants were screened for TSPO binding

Table 1
Demographics and characteristics of the study population.

Characteristic	C+ ($n = 15$)		C- ($n = 15$)		HC ($n = 13$)		Group difference	
							F/X^2	p^a
Age in years, mean (SD)	51	(8)	49	(6)	44	(11)	2.27	0.116
Education in years, mean (SD)	13	(3)	14	(3)	14	(2)	0.21	0.813
Body-mass index in kg/m^2, mean (SD)	25	(4)	25	(5)	23	(3)	1.40	0.258
Postmenopausal at diagnosis, no. (%)	9	(60)	6	(40)	–	–	0.53	0.273†
Post- or perimenopausal at assessment, no. (%)	14	(93)	6	(40)	4	(31)	13.39	**0.001†**
Days since end of chemotherapy/surgery, mean (SD)	28	(13)	36	(12)	–	–	2.79	0.106
Breast cancer stage, no. (%)							–	–
0–1	0	(0)	8	(53)	–	–	–	–
2	6	(40)	6	(40)	–	–	–	–
3	9	(60)	1	(1)	–	–	–	–
Cancer treatment, no. (%)								
Neo-adjuvant chemotherapy (EC + T)	8	(53)	–	–	–	–	–	–
Scheduled for radiotherapy	10	(67)	9	(60)	–	–	–	–
Scheduled for anti-hormone therapy	8	(53)	12	(80)	–	–	–	–
High affinity binders, no. (%)	9	(60)	7	(53)	6	(46)	0.23	0.893†
Injected activity in MBq, mean (SD)	144	(12)	144	(15)	142	(23)	0.09	0.917
FLAIR imaging features, mean mL (SD)								
WML total volume	1.63	(1.19)	1.66	(1.16)	1.63	(0.92)	0.30	0.995
WML juxtacortical	0.04	(0.08)	0.04	(0.08)	0.05	(0.10)	0.06	0.940
WML periventricular	1.24	(0.93)	1.35	(0.94)	1.17	(0.78)	0.15	0.859
WML deep white matter	0.35	(0.54)	0.27	(0.29)	0.40	(0.63)	0.26	0.774
WML infratentorial	0.00	(0.01)	0.01	(0.01)	0.01	(0.02)	0.70	0.503
Neurofilament light chain, mean pg/mL (SD)	401.4	(407.2)	19.06	(11.12)	15.03	(8.22)	59.57	**1.9E-12**

[a] Group differences tested with ANOVA for continuous variables and chi-square tests for categorical variables (last indicated by †). Abbreviations: C- = chemotherapy-naïve breast cancer patients, C+ = breast cancer patients treated with chemotherapy, HC = healthy controls, EC + T = 4 rounds of epirubicin 90 mg/m^2 + cyclophosphamide 600 mg/m^2 and 4–12 rounds of paclitaxel 80 mg/m^2, SD = standard deviation, WML = white matter lesions.

affinity via blood collection, after which those with low binding affinity were excluded. The study was conducted in accordance with the Declaration of Helsinki and was approved by the Commission for Medical Ethics UZ/KU Leuven.

2.2. PET-MR acquisition

Participants underwent PET-MR neuroimaging, which has been detailed previously [17]. Briefly, PET and MR images were simultaneously acquired on a hybrid 3 T GE SIGNA scanner (release MP26; GE Healthcare, Milwaukee, USA) using an 8-channel high resolution GE Signa MRI Brain Array (8HRBRAIN) Coil. MRI sequences included (1) a 3-dimensional volumetric sagittal T1-weighted image (3D BRAVO), (2) a zero-echo-time MR for PET attenuation correction, and (3) a 3-dimensional T2-weighted FLAIR image (FOV: $256 \times 256 \times 268$, voxel size: $1 \times 1 \times 0.7$ mm^3, TR/TE: 8400 ms/137.4 ms, flip angle: 90°). Simultaneously, 60 min dynamic PET scans were acquired in 3D list-mode after a bolus injection of [^{18}F]DPA-714 (144 ± 16 MBq), during which arterial samples were manually collected to derive the arterial input curve and parent free fraction.

2.3. Quantification of PET

To estimate neuroinflammatory levels in the brain, all participants underwent [^{18}F]DPA-714 PET. For each individual, total distribution volume (VT) parametric images were created with Logan graphical analysis (LGA) [30]. To account for brain atrophy, region-based voxel-wise partial-volume correction (PVC) [36] was performed on these V_T images (PVC-V_T)(Freesurfer v6 [37]). Details of PET image processing were described previously [17]. Given that lesions were often subtle or located close to CSF- or cortex-borders, and we aimed to estimate tracer uptake in lesions as specific as possible, PET images were not post-smoothed.

2.4. Quantification of FLAIR

Lesion volumes were quantified based on anatomical MRI scans by the 'icobrain ms' application of icometrix (https://icometrix.com/se rvices/icobrain-ms). Briefly, 3D T1 and FLAIR sequences were uploaded to a secure web-based portal. MSmetrix, a probabilistic method for lesion segmentation without requiring any training data, was then applied in a fully automated fashion [38]. This resulted in segmentations for juxtacortical, periventricular, deep white matter and infratentorial lesions (McDonald criteria [39]), as well as a bias-field-corrected FLAIR. Lesion segmentations were visually checked for accuracy by a radiologist. The output file included quantitative measurements for normalized brain volume and FLAIR lesion volume.

2.5. PET x FLAIR

Next, lesions were subtracted from white matter segmentations to create NAWM masks (as a reference area for tracer uptake) (Freesurfer v6). For the total lesion, localized lesion and NAWM masks, mean [^{18}F]DPA-714 PVC-V_T and V_T were extracted (Mrtrix3). Only lesions with ≥ 2 voxels were further processed to avoid inclusion of random hyperintense voxels. [^{18}F]DPA-714 V_T was not calculated in infratentorial lesions, because of their minimal prevalence.

2.6. Statistical analyses

All statistical analyses were performed in R version 4.0.3. Normality of the data was assessed with Shapiro–Wilk test and logarithmically transformed when non-Gaussian. The threshold of significance was set at $p < 0.05$, with Bonferroni correction for multiple testing. First, group comparisons of WML volumes were performed by one-way ANOVA. Second, [^{18}F]DPA-714 binding was compared within each group between the NAWM tissue and (total and focal) WMLs, using paired t-tests. Finally, two general linear regression models were calculated to predict 1) total FLAIR white matter hyperintensity volume and 2) PVC [^{18}F]DPA-714 VT of "inflammatory lesions" (i.e. lesions that showed higher tracer uptake than the NAWM); based on NfL serum concentration and age and additionally binder for the V_T model (high or medium affinity). Outliers were defined as observations deviating >3 interquartile range from Q1 or Q3 and removed for sensitivity analyses.

3. Results

3.1. Lesion volumes

Two healthy control FLAIR scans were excluded due to motion artefacts. When comparing total FLAIR WML volume, as well as regional juxtacortical, periventricular, deep white matter and infratentorial WML volumes, none differed between groups ($p > 0.05$, $F < 0.062$) (Fig. 1 and Table 1). After the exclusion of outliers, these results remained unchanged.

3.2. Inflammation levels within lesions

When comparing [^{18}F]DPA-714 V_T in NAWM and regional WML within individuals per group, juxtacortical lesions showed a higher V_T compared to NAWM, both for C+ patients ($p = 0.002$, $t = 5.04$, 54% mean higher) and C- patients ($p = 0.008$, $t = 3.90$, 20% mean higher) (Fig. 2 and Table 2). After PVC, these differences persisted only for C+ patients ($p = 0.005$, $t = 4.30$, 40% mean higher). After excluding the outliers, results again remained unchanged. No differences between lesion tracer uptake and NAWM were observed in HC participants.

3.3. Lesion volumes & inflammation levels predicted based on NfL

For all participants together, blood NfL concentration was not associated with total FLAIR white matter hyperintensity volume ($R^2 = 0.174$, ß $= -0.261$, t $= 1.124$, p $= 0.268$), nor with juxtacortical PVC [^{18}F]DPA-714 V_T ($R^2 = 0.342$, β $= 0.096$, t $= 2.090$, p $= 0.051$), albeit a trend is observable in the latter (Fig. 3).

4. Discussion

The present study explored the extent of leukoencephalopathy and neuroinflammation as its potential underlying mechanism in a cohort of breast cancer patients. Although no significant difference in WML burden was encountered between the groups, we detected significantly more TSPO expression, indicative of increased glial activity [40], in juxtacortical WMLs compared to the NAWM, in the chemotherapy-treated patients specifically.

4.1. White matter lesion burden was not higher in breast cancer patients after chemotherapy

While earlier case series observed leukoencephalopathy during combination chemotherapy (including 5-FU) for breast cancer [41–43], we observed no differences in lesion load shortly after ending chemotherapy compared to chemotherapy-naïve patients or healthy women. This was the case for each lesion location (periventricular, deep white matter, juxtacortical, infratentorial), as well as for the total lesion load. Our findings are in line with the few larger scale studies comparing white matter hyperintensities in chemotherapy-treated patients, compared to chemotherapy-naïve patients and healthy controls [7,8, 44]. In contrast to findings in other oncological populations, e.g. leukaemia patients [45], these results suggest no (acute) changes in lesion burden in early-stage breast cancer patients (compared to controls) after the currently applied chemotherapeutic regimens (i.e. often a combination of 5-fluorouracil, epirubicin and/or cyclophosphamide). However, comparable doses of cyclophosphamide, epirubicin and paclitaxel (in our study 4×600 mg/m^2, 4×90 mg/m^2 and 4-12 $\times$ 80 mg/m^2, respectively) did result in more WML in a twin case study, two years after completion of chemotherapy [43]. This points to the possibility of delayed induced leukoencephalopathy after treatment for breast cancer, which may only be observed after a longer period. Breast cancer patients might therefore still be at risk for accelerated WML development in later ageing stages [46]. Lastly, although we did not encounter more or larger lesions shortly after treatment, our results do not exclude the possibility of more subtle white matter changes. When investigating such subtle white matter microstructural changes, abundant research has confirmed chemotherapy-associated changes in diffusion-weighted parameters (e.g. fractional anisotropy, mean diffusivity [7,8], or more recent fixel-based parameters [17]).

4.2. Increased glial activity in white matter hyperintensities

Neuroinflammation is increasingly recognized as an early event in neurodegenerative processes [47]. In this study, elevated neuro-inflammation (estimated based on TSPO tracer uptake representing mainly astrocytic and microglial activation) was observed in juxtacortical white matter lesions, but not in periventricular/deep WM lesions, compared to the healthy WM. This finding was only the case for chemotherapy-treated breast cancer patients, suggesting that neuro-inflammation in WMLs might play a pathogenetic role in "chemobrain" rather than simply reflecting an age-related effect. Chemotherapy is known to increase pro-inflammatory cytokines [48], and activate astrocytes and microglia [49]. Given the important role of these resident immune cells in oligodendrogenesis, it was suggested that neuro-inflammation, more specifically activated microglia, could contribute to the decreased WM integrity (and consequently observable WMLs) after chemotherapy [49], which could be a potential underlying mechanism of cancer related cognitive impairment. We indeed found elevated TSPO tracer uptake in juxtacortical lesions in chemotherapy-treated patients specifically. From a pathological perspective, Moore-Maxwell et al. (2004) also demonstrated gliosis (astrocytes) and macrophage (microglial) infiltration in several post-mortem brain autopsies of former cancer patients (e.g. breast cancer) in lesioned areas (as measured on T2-weighted scans in vivo) [22]. Similar to our chemotherapy-treated
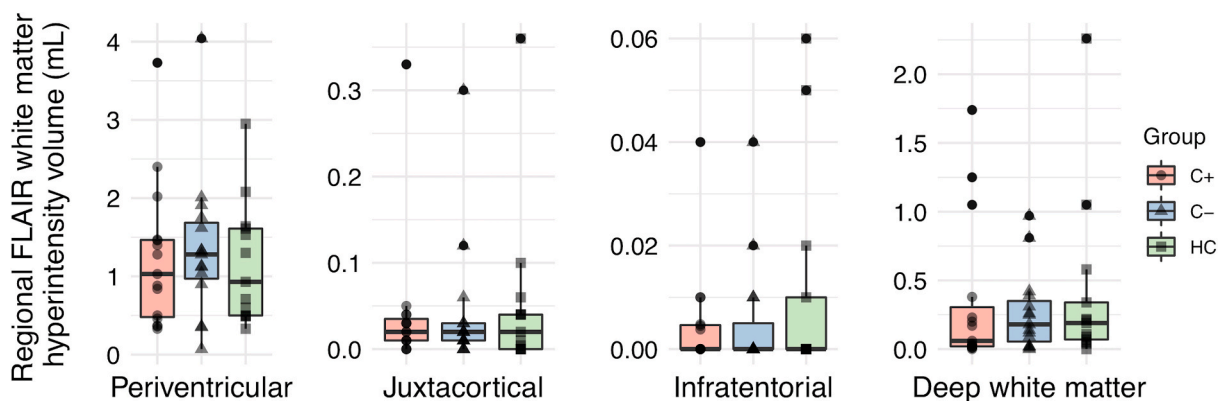

Fig. 1. Regional white matter lesion volumes. Abbreviations: C- = chemotherapy-naïve breast cancer patients, C+ = breast cancer patients treated with chemotherapy, HC = healthy controls.
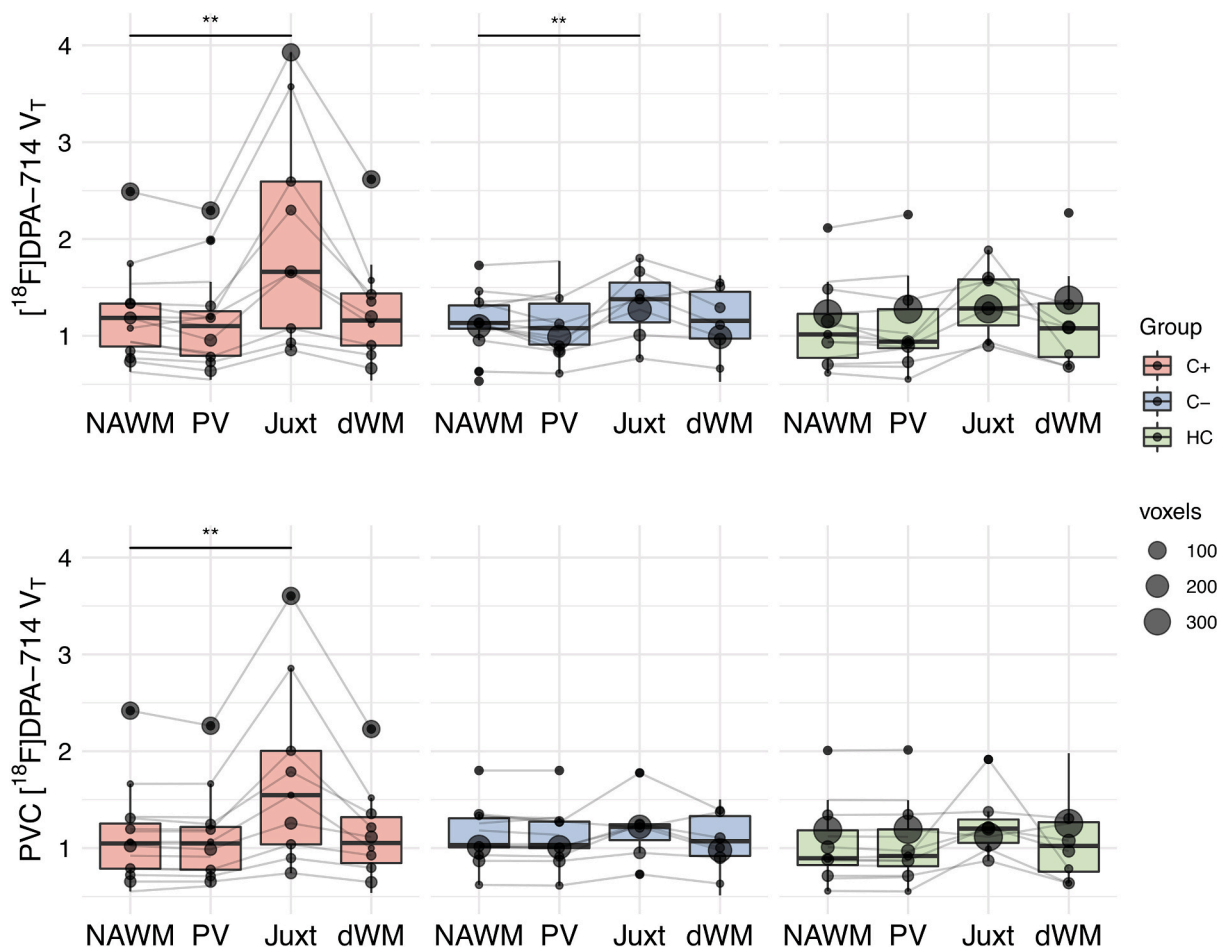
Fig. 2. [^{18}F]DPA-714 V_T in regional lesioned and normal appearing white matter. Only regions with a minimum of two voxels were evaluated. ** paired *t*-test p-value of <0.0125. Abbreviations: C- = chemotherapy-naïve breast cancer patients, C+ = breast cancer patients treated with chemotherapy, dWM = deep white matter lesions, HC = healthy controls, Juxt = juxtacortical lesions, NAWM = normal appearing white matter, PV = periventricular lesions, PVC = region-based voxel-wise partial volume corrected, V_T = total volume of distribution.

Table 2
[^{18}F]DPA-714 binding in FLAIR hyperintense regions.

PET characteristic	C+ (n = 15)		paired *t*-test		C- (n = 15)		paired *t*-test		HC (n = 13)		paired *t*-test	
			t	$p_{uncorrected}$			t	$p_{uncorrected}$			t	$p_{uncorrected}$
V_T, mean (SD)												
NAWM	1.20	(0.47)	–	–	1.14	(0.30)	–	–	1.10	(0.42)	–	–
total WML	1.17	(0.53)	1.87		1.11	(0.34)	1.54	0.145	1.09	(0.45)	0.87	0.402
periventricular WML	1.14	(0.49)	2.67	**0.018**	1.07	(0.34)	2.48	**0.026**	1.08	(0.46)	1.07	0.306
juxtacortical WML	1.91	(1.12)	5.04	**0.002***	1.33	(0.36)	3.90	**0.008***	1.42	(0.34)	2.58	**0.049**
deep white matter WML	1.23	(0.53)	0.75	0.467	1.16	(0.33)	1.54	0.146	1.13	(0.47)	0.32	0.756
PVC V_T, mean (SD)												
NAWM	1.12	(0.42)	–	–	1.09	(0.28)	–	–	1.05	(0.39)	–	–
total WML	1.12	(0.42)	1.75	0.360	1.08	(0.32)	0.97	0.345	1.05	(0.39)	0.32	0.755
periventricular WML	1.09	(0.43)	2.62	**0.020**	1.07	(0.32)	1.61	0.129	1.04	(0.39)	0.39	0.706
juxtacortical WML	1.62	(0.99)	4.29	**0.005***	1.20	(0.32)	2.86	**0.029**	1.28	(0.35)	1.86	0.122
deep white matter WML	1.12	(0.43)	0.23	0.821	1.07	(0.29)	0.52	0.613	1.06	(0.40)	0.08	0.932

Only regions with a minimum of two voxels were evaluated. * Surviving Bonferonni correction for comparing four outcomes (p < 0.0125).
Abbreviations: C- = chemotherapy-naïve breast cancer patients, C+ = breast cancer patients treated with chemotherapy, FLAIR = fluid attenuated inversion recovery sequence, HC = healthy controls, PET = positron emission tomography, PVC = region-based voxel-wise partial volume corrected, SD = standard deviation, V_T = total volume of distribution, WML = white matter lesions, observed as hyperintense regions on FLAIR magnetic resonance imaging.

breast cancer population, increased glial expression in WMLs was also found in MS [34] and in natalizumab-induced progressive multifocal leukoencephalopathy [50], suggesting similar immune pathways to be involved.

Of note, this effect was only encountered in juxtacortical lesions, not in periventricular nor deep white matter. This could possibly be attributed to the different white matter microstructure of these different regions. More specifically, juxtacortical white matter areas have U-fibers (i.e. short association fibers), rather than long white matter tracts [51]. Furthermore, these areas myelinate later (i.e. 3rd-4th decade) than periventricular or deep white matter. Hence, the observed higher inflammation in juxtacortical lesions could possibly be explained by
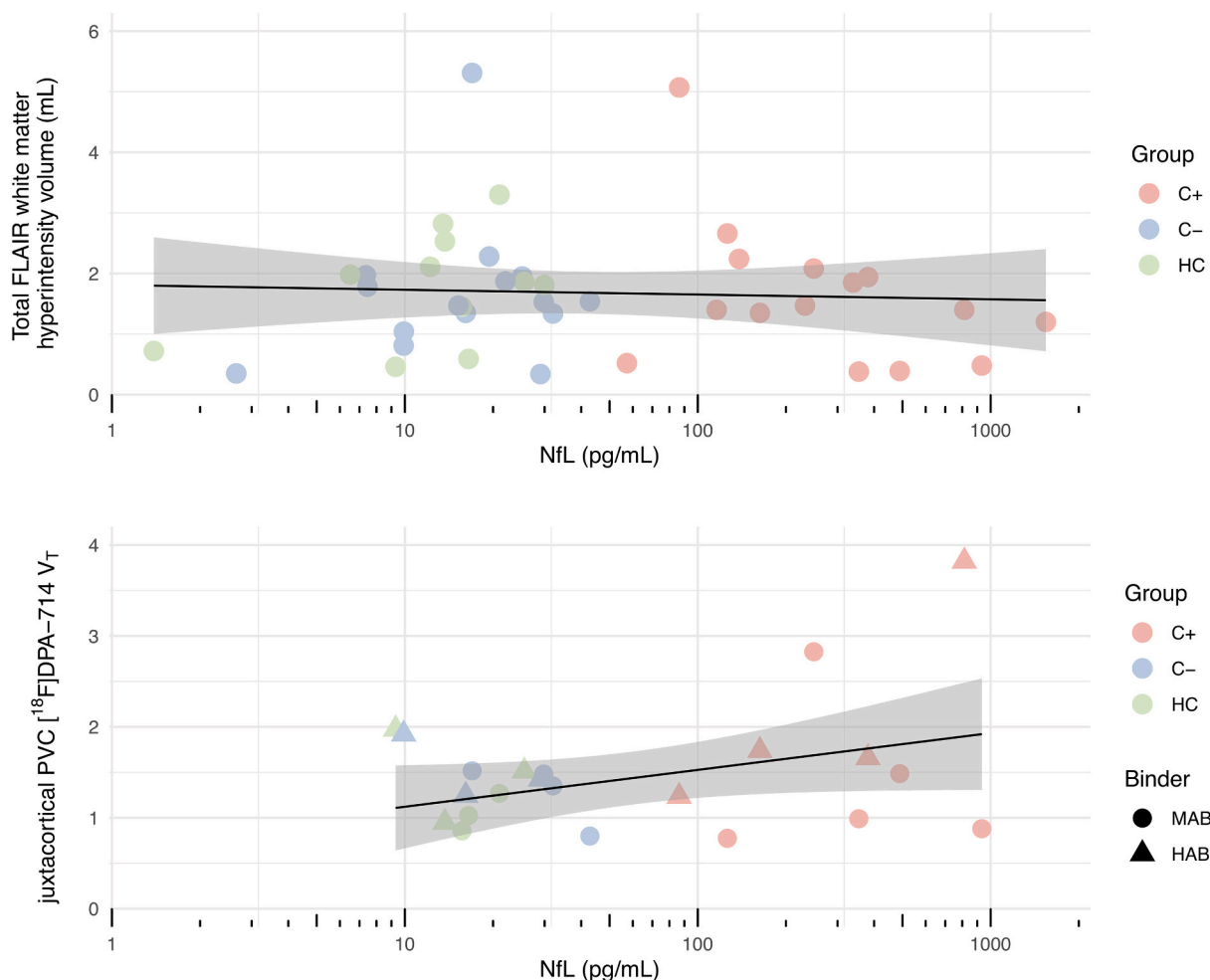
Fig. 3. Total white matter lesion volume and juxtacortical glial activation and their linear relationship with blood NfL concentration. Only juxtacortical regions with a minimum of two voxels were evaluated. No associations were found ($R^2 < 0.342$, $p > 0.05$). Lines represent linear regression lines with shaded 95% confidence intervals. Abbreviations: C- = chemotherapy-naïve breast cancer patients, C+ = breast cancer patients treated with chemotherapy, HAB = high affinity binder, HC = healthy controls, MAB = medium affinity binder, NfL = neurofilament-light chain, PVC = region-based voxel-wise partial volume corrected, V_T = total volume of distribution.

damage to oligodendroglia, rather than changes in myelin metabolism/turnover, as these U-fibers only have a slow metabolism rate (compared to periventricular and deep white matter areas) [52]. Such damage to oligodendroglia preceded by microglial activation was recently suggested by Gibson and Monje (2019) [13,49]. This study is the first *in vivo* study in humans supporting this hypothesis, more specifically in juxtacortical areas in early-stage breast cancer patients after chemotherapy.

4.3. Glial activity in juxtacortical lesions not associated with NfL

In our previous work, we observed higher NfL serum levels in chemotherapy-treated patients as well as a positive relationship between NfL concentration and relative glial activation in grey matter brain regions, indicating an association between neurotoxic and neuroinflammatory processes in (sub)cortical regions [17]. Additionally, recent research in MS patients observed a microglia-specific protein, measured from CSF, to be associated with NfL [32]. Moreover, this inflammation-related protein was associated with total lesion volume three years later, while this was not the case for NfL.

By contrast, in this study, we did not observe a significant association between juxtacortical white matter glial activation and NfL serum levels shortly after chemotherapy for breast cancer. Still, a trend of a linear relationship was observable, and the effect was borderline non-

significant. Future studies with a larger sample size could validate whether this relationship would be confirmed. A possible explanation why NfL levels were earlier associated with cortical inflammation [17], but not inflammation in juxtacortical lesions, could be that tracer uptake in the white matter is generally lower and less specific. Moreover, in the aforementioned MS study (30), NfL was extracted from CSF instead of blood, which could also contribute to the lack of association with lesion inflammation in our study [32]. Combined with our findings of lesion loads being in the range of normal ageing, our results suggest that increased neuroinflammation in white (and grey) matter potentially precedes induced WM lesions, rather than simultaneously co-occurring. Such order of mechanisms (i.e. inflammation, oligodendroglial cell damage) as earlier suggested could also support the hypothesis of NfL to change only after initial inflammation (rather than simultaneously). In MS patients NfL indeed appeared to be an initial precursor of observable lesions at a later timepoint [15]. Confirmation of such time-dependent changes in oncological populations however requires longitudinal investigations to be conducted.

4.4. Limitations and future directions

The largest strength of this study is the use of the highly specific second-generation TSPO tracer [18F]DPA-714, which allowed us to study glial activation (e.g. neuroinflammation) *in vivo*. However,

interpreting the cellular specificity of the TSPO signal still warrants caution, since it can be driven by other factors such as expression on astrocytes or endothelial cells, recruitment of monocytes and changes in BBB permeability [53,54]. Currently, the best way to circumvent such obstacles relies on kinetic modelling through use of the metabolite-corrected arterial input function, as applied in this study. However, the results of this pilot study should still be considered preliminary and exploratory because of the small sample size and cross-sectional design. For instance, lesions were not observed in all participants and juxtacortical lesions were generally small, often including a limited number of voxels, which could have influenced our findings. Additionally, as TSPO uptake is known to be higher in grey matter and consequently cortical regions [55], the higher juxtacortical lesion uptake could partly be enhanced by cortical spill-over. However, partial volume correction was applied to improve quantitative accuracy of regional PET signal, which is assumed to provide a more reliable representation of the underlying inflammation values [36]. Furthermore, lesions were stringently checked for accuracy by a radiologist and imaging maps were corrected (only including the white matter). While our results persisted after these corrections, additional research will be necessary to confirm our findings. Lastly, since clinical characteristics inherently differ between patient groups, differences observed between patients cannot solely be attributed to treatment with chemotherapy, but most likely reflect a combination of individual susceptibility, disease status and subsequent treatment regime. Additionally, cardiovascular risk factors for instance are known to influence presentation of white matter hyperintensities on FLAIR images [56]. While groups were matched for age and participants were excluded if a history of cerebrovascular disease was known, other comorbidities such as obesity, hypertension, diabetes mellitus and/or smoking could also have influenced our results and therefore require further exploration.

Further studies are needed to confirm the interplay between leukoencephalopathy and neuroinflammation in cancer populations. Our cross-sectional findings support the hypothesis that microglial activity precedes WMLs, but this can only be validated by combining both imaging modalities over time. For instance, future research involving a larger cohort of (breast) cancer patients who are longitudinally followed with PET-MR imaging (e.g. evaluating subtle changes in longitudinal lesion volumes, longitudinal PET acquisition with less invasive tracer quantification [57] or more refined measurements of white matter microstructure such as diffusion-weighted MRI), will yield important results concerning observable leukoencephalopathy and its underlying mechanisms in cancer survivors. While we did not observe associations between NfL and leukoencephalopathy, earlier studies employing NfL derived from CSF in other populations did [32], suggesting such values could prove important biomarkers in future studies of populations who receive CSF extraction in their clinical follow-up (e.g. leukaemia).

5. Conclusion

Based on this cross-sectional study, innate immune cell activation is suggested to possibly be involved in the development of juxtacortical WMLs after chemotherapy for early-stage breast cancer. This is the first study estimating neuroinflammation in WMLs in this population *in vivo*, using TSPO [^{18}F]DPA714-PET and automated lesion delineations. Although lesion burden was not larger in patients compared to controls, inflammation might precede lesion development after longer time intervals, or be associated with more subtle changes in the white matter microstructure. Longitudinal and preclinical studies are required to validate these hypotheses and the time-dependency of specific toxic events.

Funding

Declaration of competing interest

The authors report to have no conflict of interest.

References

[1] Bray F, Ferlay J, Soerjomataram I, Siegel RL, Torre LA, Jemal A. Global cancer statistics 2018: GLOBOCAN estimates of incidence and mortality worldwide for 36 cancers in 185 countries. CA Canc J Clin 2018. https://doi.org/10.3322/caac.21492.

[2] Sousa H, Almeida S, Bessa J, Pereira MG. The developmental trajectory of cancer-related cognitive impairment in breast cancer patients: a systematic review of longitudinal neuroimaging studies. Neuropsychol Rev 2020. https://doi.org/10.1007/s11065-020-09441-9.

[3] Dijkshoorn ABC, van Stralen HE, Sloots M, Schagen SB, Visser-Meily JMA, Schepers VPM. Prevalence of cognitive impairment and change in patients with breast cancer: a systematic review of longitudinal studies. Psychooncology 2021. https://doi.org/10.1002/pon.5623.

[4] Deprez S, Amant F, Smeets A, Peeters R, Leemans A, Van Hecke W, et al. Longitudinal assessment of chemotherapy-induced structural changes in cerebral white matter and its correlation with impaired cognitive functioning. J Clin Oncol 2012;30:274–81. https://doi.org/10.1200/JCO.2011.36.8571.

[5] Deprez S, Amant F, Yigit R, Porke K, Verhoeven J, Stock J Van den, et al. Chemotherapy-induced structural changes in cerebral white matter and its correlation with impaired cognitive functioning in breast cancer patients. Hum Brain Mapp 2011;32:480–93. https://doi.org/10.1002/hbm.21033.

[6] Abraham J, Haut MW, Moran MT, Filburn S, Lemiuex S, Kuwabara H. Adjuvant chemotherapy for breast cancer: effects on cerebral white matter seen in diffusion tensor imaging. Clin Breast Cancer 2008;8:88–91.

[7] De Ruiter MB, Reneman L, Boogerd W, Veltman DJ, Caan M, Douaud G, et al. Late effects of high-dose adjuvant chemotherapy on white and gray matter in breast cancer survivors: converging results from multimodal magnetic resonance imaging. Hum Brain Mapp 2012;33:2971–83. https://doi.org/10.1002/hbm.21422.

[8] Stouten-Kemperman MM, de Ruiter MB, Koppelmans V, Boogerd W, Reneman L, Schagen SB. Neurotoxicity in breast cancer survivors ≥10 years post-treatment is dependent on treatment type. Brain Imaging Behav 2015;9:275–84. https://doi.org/10.1007/s11682-014-9305-0.

[9] Bolton G, Isaacs A. Women's experiences of cancer-related cognitive impairment, its impact on daily life and care received for it following treatment for breast cancer. Psychol Health Med 2018. https://doi.org/10.1080/13548506.2018.1500023.

[10] Schroyen G, Vissers J, Smeets A, Gillebert CR, Lemiere J, Sunaert S, et al. Blood and neuroimaging biomarkers of cognitive sequelae in breast cancer patients throughout chemotherapy: a systematic review. Transl Oncol 2022;16:101297. https://doi.org/10.1016/J.TRANON.2021.101297.

[11] Miron VE, Kuhlmann T, Antel Jack PJP. Cells of the oligodendroglial lineage, myelination, and remyelination. Biochim Biophys Acta - Mol Basis Dis 2011. https://doi.org/10.1016/j.bbadis.2010.09.010.

[12] Brugulat-Serrat A, Salvadó G, Operto G, Cacciaglia R, Sudre CH, Grau-Rivera O, et al. White matter hyperintensities mediate gray matter volume and processing speed relationship in cognitively unimpaired participants. Hum Brain Mapp 2020. https://doi.org/10.1002/hbm.24877.

[13] Gibson EM, Monje M. Emerging mechanistic underpinnings and therapeutic targets for chemotherapy-related cognitive impairment. Curr Opin Oncol 2019. https://doi.org/10.1097/CCO.0000000000000578.

[14] Ashton NJ, Janelidze S, Al Khleifat A, Leuzy A, van der Ende EL, Karikari TK, et al. A multicentre validation study of the diagnostic value of plasma neurofilament light. Nat Commun 2021;12:3400. https://doi.org/10.1038/s41467-021-23620-z.

[15] Kuhle J, Kropshofer H, Haering DA, Kundu U, Meinert R, Barro C, et al. Blood neurofilament light chain as a biomarker of MS disease activity and treatment response. Neurology 2019. https://doi.org/10.1212/WNL.0000000000007032.

[16] Natori A, Ogata T, Sumitani M, Kogure T, Yamauchi T, Yamauchi H. Potential role of pNF-H, a biomarker of axonal damage in the central nervous system, as a predictive marker of chemotherapy-induced cognitive impairment. Clin Cancer Res 2015;21:1348–52. https://doi.org/10.1158/1078-0432.CCR-14-2775.

[17] Schroyen G, Blommaert J, van Weehaeghe D, Sleurs C, Vandenbulcke M, Dedoncker N, et al. Neuroinflammation and its association with cognition, neuronal markers and peripheral inflammation after chemotherapy for breast cancer. Cancers (Basel) 2021;13.

[18] Ruiter MB de, Reneman L, Kieffer JM, Oldenburg HSA, Schagen SB. Brain white matter microstructure as a risk factor for cognitive decline after chemotherapy for breast cancer. Https://DoiOrg/101200/JCO2100627 2021. https://doi.org/10.1200/JCO.21.00627.

[19] Billiet T, Emsell L, Vandenbulcke M, Peeters R, Christiaens D, Leemans A, et al. Recovery from chemotherapy-induced white matter changes in young breast cancer survivors? Brain Imaging Behav 2017;1–14. https://doi.org/10.1007/s11682-016-9665-8.

[20] Schroyen G, Meylaers M, Deprez S, Blommaert J, Smeets A, Jacobs S, et al. Prevalence of leukoencephalopathy and its potential cognitive sequelae in cancer patients. J Chemother 2020:1–17. https://doi.org/10.1080/1120009X.2020.1805239.

[21] Matsos A, Loomes M, Zhou I, Macmillan E, Sabel I, Rotziokos E, et al. Chemotherapy-induced cognitive impairments: white matter pathologies. Cancer Treat Rev; 2017. https://doi.org/10.1016/j.ctrv.2017.09.010.

[22] Moore-Maxwell CA, Datto MB, Hulette CM. Chemotherapy-induced toxic leukoencephalopathy causes a wide range of symptoms: a series of four autopsies. Mod Pathol 2004. https://doi.org/10.1038/modpathol.3800049.

[23] Koppelmans V, Vernooij MW, Boogerd W, Seynaeve C, Ikram MA, Breteler MMB, et al. Prevalence of cerebral small-vessel disease in long-term breast cancer survivors exposed to both adjuvant radiotherapy and chemotherapy. J Clin Oncol 2015;33:588–93. https://doi.org/10.1200/JCO.2014.56.8345.

[24] Ahles TA, Saykin AJ. Candidate mechanisms for chemotherapy-induced cognitive changes. Nat Rev Cancer 2007;7:192–201. https://doi.org/10.1038/nrc2073.

[25] Seigers R, Fardell JE. Neurobiological basis of chemotherapy-induced cognitive impairment: a review of rodent research. Neurosci Biobehav Rev 2011;35:729–41. https://doi.org/10.1016/j.neubiorev.2010.09.006.

[26] Seigers R, Timmermans J, Van Der Horn HJ, De Vries EFJ, Dierckx RA, Visser L, et al. Methotrexate reduces hippocampal blood vessel density and activates microglia in rats but does not elevate central cytokine release. Behav Brain Res 2010;207:265–72. https://doi.org/10.1016/j.bbr.2009.10.009.

[27] Yao R, Pan R, Shang C, Li X, Cheng J, Xu J, et al. Translocator protein 18 kDa (TSPO) deficiency inhibits microglial activation and impairs mitochondrial function. Front Pharmacol 2020. https://doi.org/10.3389/fphar.2020.00986.

[28] Peyronneau MA, Saba W, Goutal S, Damont A, Dollé F, Kassiou M, et al. Metabolism and quantification of [18F]DPA-714, a new TSPO positron emission tomography radioligand. Drug Metab Dispos 2013. https://doi.org/10.1124/dmd.112.046342.

[29] Van Weehaeghe D, Babu S, De Vocht J, Zürcher N, Chew S, Cj T, et al. Moving toward multicenter therapeutic trials in amyotrophic lateral sclerosis: feasibility of data pooling using different translocator protein PET radioligands. J Nucl Med 2020;61:1621–7. https://doi.org/10.2967/JNUMED.119.241059.

[30] Lavisse S, García-Lorenzo D, Peyronneau MA, Bodini B, Thiriez C, Kuhnast B, et al. Optimized quantification of translocator protein radioligand 18F-DPA-714 uptake in the brain of genotyped healthy volunteers. J Nucl Med 2015;56:1048–54. https://doi.org/10.2967/jnumed.115.156083.

[31] Briones TL, Woods J. Dysregulation in myelination mediated by persistent neuroinflammation: possible mechanisms in chemotherapy-related cognitive impairment. Brain Behav Immun 2014;35:23–32. https://doi.org/10.1016/j.bbi.2013.07.175.

[32] Oldoni E, Smets I, Mallants K, Vandebergh M, Van Horebeek L, Poesen K, et al. CHIT1 at diagnosis reflects long-term multiple sclerosis disease activity. Ann Neurol 2020;87:633–45. https://doi.org/10.1002/ana.25691.

[33] Datta G, Colasanti A, Rabiner EA, Gunn RN, Malik O, Ciccarelli O, et al. Neuroinflammation and its relationship to changes in brain volume and white matter lesions in multiple sclerosis. Brain 2017. https://doi.org/10.1093/brain/awx228.

[34] Sucksdorff M, Matilainen M, Tuisku J, Polvinen E, Vuorimaa A, Rokka J, et al. Brain TSPO-PET predicts later disease progression independent of relapses in multiple sclerosis. Brain 2020. https://doi.org/10.1093/brain/awaa275.

[35] Nutma E, Stephenson JA, Gorter RP, De Bruin J, Boucherie DM, Donat CK, et al. A quantitative neuropathological assessment of translocator protein expression in multiple sclerosis. Brain 2019. https://doi.org/10.1093/brain/awz287.

[36] Thomas BA, Erlandsson K, Modat M, Thurfjell L, Vandenberghe R, Ourselin S, et al. The importance of appropriate partial volume correction for PET quantification in Alzheimer's disease. Eur J Nucl Med Mol Imag 2011;38:1104–19. https://doi.org/10.1007/s00259-011-1745-9.

[37] Fischl B. FreeSurfer Neuroimage 2012;62:774–81. https://doi.org/10.1016/j.neuroimage.2012.01.021.

[38] Jain S, Sima DM, Ribbens A, Cambron M, Maertens A, Hecke W Van, et al. Automatic segmentation and volumetry of multiple sclerosis brain lesions from MR images. Neuroimage (Amst) 2015;8:367. https://doi.org/10.1016/J.NICL.2015.05.003.

[39] Polman CH, Reingold SC, Banwell B, Clanet M, Cohen JA, Filippi M, et al. Diagnostic criteria for multiple sclerosis: 2010 Revisions to the McDonald criteria. Ann Neurol 2011;69:292–302. https://doi.org/10.1002/ANA.22366.

[40] Beckers L, Ory D, Geric I, Declercq L, Koole M, Kassiou M, et al. Increased expression of translocator protein (TSPO) marks pro-inflammatory microglia but does not predict neurodegeneration. Mol Imag Biol 2018. https://doi.org/10.1007/s11307-017-1099-1.

[41] Choi SM, Lee SH, Yang YS, Kim BC, Kim MK, Cho KH. 5-fluorouracil-induced leukoencephalopathy in patients with breast cancer. J Kor Med Sci 2001;16:328–34. https://doi.org/10.3346/jkms.2001.16.3.328.

[42] Brown MS, Stemmer SM, Simon JH, Stears JC, Jones RB, Cagnoni PJ, et al. White matter disease induced by high-dose chemotherapy: longitudinal study with MR imaging and proton spectroscopy. Am J Neuroradiol 1998;19:217–21.

[43] Ferguson RJ, McDonald BC, Saykin AJ, Ahles TA. Brain structure and function differences in monozygotic twins: possible effects of breast cancer chemotherapy. J Clin Oncol 2007;25:3866–70. https://doi.org/10.1200/JCO.2007.10.8639.

[44] Koppelmans V, de Groot M, de Ruiter MB, Boogerd W, Seynaeve C, Vernooij MW, et al. Global and focal white matter integrity in breast cancer survivors 20 years after adjuvant chemotherapy. Hum Brain Mapp 2014;35:889–99. https://doi.org/10.1002/hbm.22221.

[45] Rijmenams I, Moechars D, Uyttebroeck A, Radwan A, Blommaert J, Deprez S, et al. Age-and intravenous methotrexate-associated leukoencephalopathy and its neurological impact in pediatric patients with lymphoblastic leukemia. Cancers (Basel) 2021. https://doi.org/10.3390/cancers13081939.

[46] Carlson BW, Craft MA, Carlson JR, Razaq W, Deardeuff KK, Benbrook DM. Accelerated vascular aging and persistent cognitive impairment in older female breast cancer survivors. GeroScience 2018. https://doi.org/10.1007/s11357-018-0025-z.

[47] Schain M, Kreisl WC. Neuroinflammation in neurodegenerative disorders—a review. Curr Neurol Neurosci Rep 2017;17:25. https://doi.org/10.1007/s11910-017-0733-2.

[48] Castel H, Denouel A, Lange M, Tonon M-C, Dubois M, Joly F. Biomarkers associated with cognitive impairment in treated cancer patients: potential predisposition and risk factors. Front Pharmacol 2017;8:138. https://doi.org/10.3389/fphar.2017.00138.

[49] Em G, M M. Microglia in cancer therapy-related cognitive impairment. Trends Neurosci 2021;44:441–51. https://doi.org/10.1016/J.TINS.2021.02.003.

[50] Mahler C, Schumacher A-M, Unterrainer M, Kaiser L, Höllbacher T, Lindner S, et al. TSPO PET imaging of natalizumab-associated progressive multifocal leukoencephalopathy. Brain 2021. https://doi.org/10.1093/brain/awab127.

[51] Kim KW, MacFall JR, Payne ME. Classification of white matter lesions on magnetic resonance imaging in elderly persons. Biol Psychiatr 2008. https://doi.org/10.1016/j.biopsych.2008.03.024.

[52] Paul RH, editor. Vascular dementia: cerebrovascular mechanisms and clinical management; 2005.

[53] Kreisl WC, Kim MJ, Coughlin JM, Henter ID, Owen DR, Innis RB. PET imaging of neuroinflammation in neurological disorders. Lancet Neurol 2020;19:940–50. https://doi.org/10.1016/S1474-4422(20)30346-X.

[54] Owen DR, Narayan N, Wells L, Healy L, Smyth E, Rabiner EA, et al. Pro-inflammatory activation of primary microglia and macrophages increases 18 kDa translocator protein expression in rodents but not humans. J Cerebr Blood Flow Metabol 2017;37:2679–90. https://doi.org/10.1177/0271678X17710182.

[55] Arlicot N, Vercouillie J, Ribeiro M-J, Tauber C, Venel Y, Baulieu J-L, et al. Initial evaluation in healthy humans of [18F]DPA-714, a potential PET biomarker for neuroinflammation. Nucl Med Biol 2012;39:570–8. https://doi.org/10.1016/j.nucmedbio.2011.10.012.

[56] Fuhrmann D, Nesbitt D, Shafto M, Rowe JB, Price D, Gadie A, et al. Strong and specific associations between cardiovascular risk factors and white matter micro-and macrostructure in healthy aging. Neurobiol Aging 2019;74:46–55. https://doi.org/10.1016/J.NEUROBIOLAGING.2018.10.005.

[57] Mertens N, Schmidt ME, Hijzen A, Van Weehaeghe D, Ravenstijn P, Depre M, et al. Minimally invasive quantification of cerebral P2X7R occupancy using dynamic [18F]JNJ-64413739 PET and MRA-driven image derived input function. 2021 111 Sci Rep 2021. https://doi.org/10.1038/s41598-021-95715-y. 11:1–11.